AU J.T. 15(4): 253-259 (Apr. 2012)

A 9-*dof* Displacement Analysis of a Large Truck Plying a Rough Road

Akinola Abdul-Ghaniyu Adeniyi and Abubakar Mohammed*

Mechanical Engineering Department, University of Ilorin, Ilorin, Kwara State, Nigeria
E-mail: <adeniyi.aa@unilorin.edu.ng>

Abstract

We present a 9-degree of freedom analysis of a 2D truck with the assumption that the coefficient of damping can be modelled as proportion to the stiffness matrix. There are nine modes of vibrations observed. The modes of vibration show that the articulated vehicle un-sprung masses move in different phases relative to one another in the modes. A driving comfort measured by the impact response in the driver cabin for the selected stiffness matrix is only 1.32% relative to acceleration of gravity. The sinusoidal road profile gives an oscillating response in the trailer compartment which settles to a sinusoidal amplitude of 0.5^o from an initial 1.5^o amplitude, while the driver cabin oscillation is only 0.02^o. This is a comfortable ride without consideration for seat ergonomics and the physiological effect of low frequency vibration and long time driving.

Keywords: *Damping, vibration, coefficient of damping, stiffness matrix.*

Introduction

A commercial truck has several sophisticated suspension systems aimed at providing smooth driving and comfort and protecting the machinery and the goods or equipment transported. There are a number of literatures which show interest of researchers in ride comfort (Hać̒ 1985; Ikenaga *et al*. 2000; Jie *et al*. 2011; Fan *et al*. 2011). A review by Mabbott *et al*. (2001) suggests that low frequency vibration may be associated with driver fatigue.

Programmers developing a computer based game or simulator application for vehicle driven on some road profile can make more realistic motion by understanding the dynamics and vibration modes of such vehicles but for a more realistic virtual reality simulator of a vehicle, a 3D model would provide better results.

Maeda *et al*. (2005), in the vehicle simulator validation research, noted that road design requires understanding vehicle response to road profile.

2D Truck Model

The representative 2D truck model of Fig. 1 is used in this analysis. To reduce the complexity of the system of equations, the damping coefficients are assumed to be linearly proportional to the stiffness by a factor of proportionality.

Similar to the 4-*dof* (degree of freedom) simplification in Hedrick and Butsuen (1990), the system is modelled as shown in Fig. 2 without the dampers. Also, the un-sprung masses are considered as rigid bodies.

It is also assumed that the road excitation could be represented analytically. Other techniques are possible for representing a road profile, direct data measurement from the road or spectral density method as in the review by Jiang *et al*. (2001) but a simple sinusoidal representation of the form $F = \bar{F} e^{-j \omega t}$ is used here for simplicity.

* Mechanical Engineering Department, Federal University of Technology, Minna, Niger State, Nigeria.
E-mail: <a.mohammed@futminna.edu.ng>.

The effects of friction and tyre pressure discussed by M'Sirdi *et al*. (2005) would only unnecessarily complicate the computation for this analysis and such effects are factored into the forcing functions:

$F_1 = k_5\, y_1$, (1)

$F_2 = k_6\, y_2$, and (2)

$F_3 = k_9\, y_3$. (3)

The road profile is described in the form:

$y_r = A\sin(\omega t - (2\pi/\lambda)X_r)$ (4)

where: X_r is the wheel coordinate relative to the front wheel; t is the time; ω is the angular frequency, ω = 10.472 rad/s; λ is the wavelength; and A = 0.1 m.

Forces F_1, F_2 and F_3 are the road excitations at the wheels of the articulated vehicle. The close wheels have been combined as single wheels for simplicity as shown in Fig. 2. The three un-sprung masses are allowed to tilt about their individual centre of mass and can make vertical oscillations. The degrees of freedom (*dof*) are x_j for the linear displacements and j ranges from 1 to 6; the angular *dof* are θ_1, θ_2, and θ_3. To ensure that the variables are not linearly dependent, the following variables are adopted and have been used in the motion equations:

$y_1 = x_2 + l_3\theta_2$, $y_5 = x_2 - l_6\theta_2$,

$y_2 = x_2 + l_5\theta_2$, $y_6 = x_1 + l_1\theta_1$,

$y_3 = x_2 - l_4\theta_2$, $y_7 = x_1 - l_2\theta_1$,

$y_4 = x_2 - l_7\theta_2$, $y_8 = x_5 + l_8\theta_3$, and

$y_9 = x_5 - l_9\theta_3$.

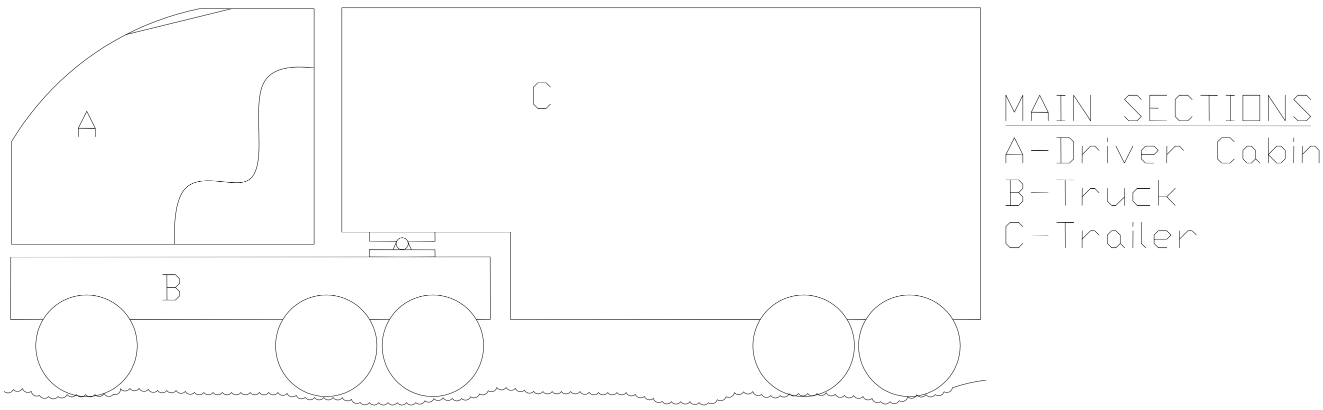

Fig. 1. A representative 2D truck model.

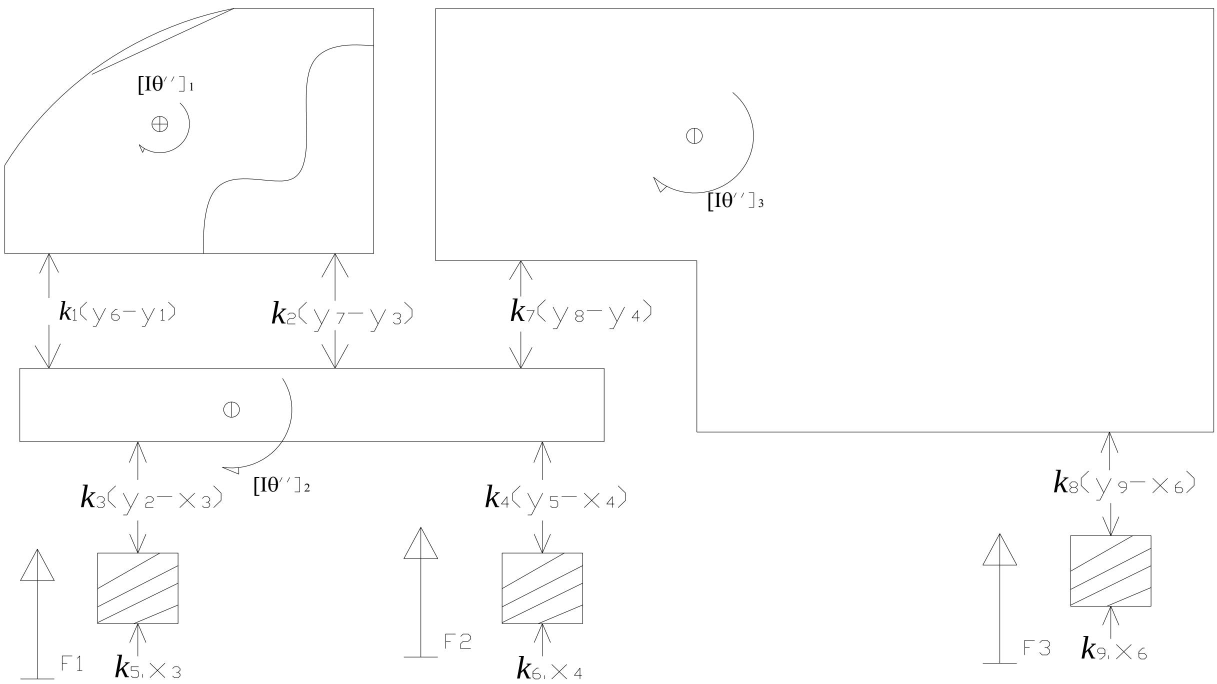

Fig. 2. Dynamic model of the truck system.

The solution method follows the Lagrange-d'Alembert's principles. The equation of motion is of the form

$$m\ddot{x} + \alpha k\dot{x} + kx = F. \quad (5)$$

In forming the equations, the next equation form has been used:

$$m\ddot{x} + kx = F. \quad (6)$$

where: m represents mass; k represents stiffness; αk is the damping coefficient; α is a factor of proportionality; and F is the excitation force. Figure 2 is used to resolve the sets of equations following.

If the cabin has a mass m_1 and moment of inertia I_1, then the motion equation is:

$$m_1\ddot{x}_1 + k_1(y_6 - y_1) + k_2(y_7 - y_3) = 0,$$

$$m_1\ddot{x}_1 + x_1(k_1 + k_2) - x_2(k_1 + k_2) + \theta_1(k_1l_1 - k_2l_2) + \theta_2(k_2l_4 - k_1l_3) = 0. \quad (7)$$

The trailer unit having mass m_5 and moment of inertia I_3 can be represented as:

$$m_5\ddot{x}_5 + k_7(y_8 - y_4) + k_8(y_9 - x_6) = 0,$$

$$m_5\ddot{x}_5 - x_2k_7 + x_5(k_7 + k_8) - x_6k_8 + \theta_2k_7l_7 + \theta_3(k_7l_8 - k_8l_9) = 0. \quad (8)$$

The motion of the engine chassis, which has a combined mass of m_2 and moment of inertia I_2, is represented in Eq. (9):

$$m_2\ddot{x}_2 + k_3(y_2 - x_3) + k_4(y_5 - x_4) - k_1(y_6 - y_1) - k_2(y_7 - y_3) - k_7(y_8 - y_4) = 0,$$

$$m_2\ddot{x}_2 - x_1(k_1 + k_2) - x_2(k_1 + k_2 + k_3 + k_4 + k_7) - x_3k_3 - x_4k_4 - x_5k_7 + \theta_1(-k_1l_1 + k_2l_2) + \theta_2(k_3l_5 - k_4l_6 + k_1l_3 - k_2l_4 - k_7l_7) - \theta_3k_7k_8 = 0. \quad (9)$$

The front wheel un-sprung mass m_3 has road excitation F_1. Its equation of motion is shown in Eq. (10):

$$m_3\ddot{x}_3 + k_5x_3 - k_3(y_2 - x_3) = F_1,$$

$$m_3\ddot{x}_3 - x_2k_3 + x_3(k_3 + k_5) - \theta_2k_3l_5 = F_1. \quad (10)$$

Similarly, the rear wheel of the truck is has un-sprung mass m_4, and excited with road excitation F_2, its motion equation shown in Eq. (11):

$$m_4\ddot{x}_4 + k_6x_4 - k_4(y_5 - x_4) = F_2,$$

$$m_4\ddot{x}_4 - x_2k_4 + x_4(k_4 + k_6) - \theta_2k_4l_6 = F_2. \quad (11)$$

For the trailer wheels with un-sprung mass m_6, and road excitation F_3, Equation (12) represents the motion:

$$m_6\ddot{x}_6 + k_9x_6 - k_8(y_9 - x_6) = F_3,$$

$$m_6\ddot{x}_6 - x_5k_8 + x_6(k_8 + k_9) - \theta_3k_8l_9 = F_3. \quad (12)$$

Taking moments about the respective centre of mass of the three un-sprung masses give the next 3 sets of equations:

$$I_1\ddot{\theta}_1 + x_1(k_1l_1 - k_2l_2) + x_2(-k_1l_1 + k_2l_2) + \theta_1(k_1l_1^2 + k_2l_2^2) - \theta_2(k_1l_1l_3 + k_2l_2l_4) = 0, \quad (13)$$

$$I_2\ddot{\theta}_2 + x_1(k_2l_4 - k_1l_3) + x_2(k_3l_5 - k_2l_4 - k_7l_7 - k_4l_6 + k_1l_3) - x_3(k_3l_5) + x_4(k_4l_6) + x_5(k_7l_7) - \theta_1(k_2l_2l_4 + k_1l_1l_3) + \theta_2(k_3l_5^2 + k_2l_4^2 + k_7l_7^2 + k_4l_6^2 + k_1l_3^2) + \theta_3(k_7l_7l_8) = 0, \quad (14)$$

$$I_3\ddot{\theta}_3 - x_2(k_7l_8) + x_5(k_7l_8 - k_8l_9) + x_6(k_8l_9) + \theta_2(k_7l_7l_8) + \theta_3(k_7l_8^2 + k_8l_9^2) = 0. \quad (15)$$

Simulation Condition and Method

The vehicle is assumed to be moving at a velocity of 60 km/hr and the road roughness is assumed to have a wavelength of 10 m, this represents a roughness of 10.47 rad/s. System response (Singiresu 2004) is obtained by solving the matrix of Eq. (17) below which is also expressed as the following Eq. (16):

$$\ddot{x} = \frac{[F]}{M} - \frac{[C]}{M}\dot{x} - \frac{[K]}{M}x, \quad (16)$$

and solved using MATLAB built-in Runge-Kunta ODE23 function, where: C represents the damping coefficient matrix; F is the forcing function matrix; and M represents the diagonal mass matrix. The dimensions and stiffness data have been adapted from Elmadany (1987) as shown in Table 1.

The solution matrix in Eq. (17) has been formed using Eq. (5).

$$\begin{bmatrix} m_1 & 0 & 0 & 0 & 0 & 0 & 0 & 0 & 0 \\ 0 & m_2 & 0 & 0 & 0 & 0 & 0 & 0 & 0 \\ 0 & 0 & m_3 & 0 & 0 & 0 & 0 & 0 & 0 \\ 0 & 0 & 0 & m_4 & 0 & 0 & 0 & 0 & 0 \\ 0 & 0 & 0 & 0 & m_5 & 0 & 0 & 0 & 0 \\ 0 & 0 & 0 & 0 & 0 & m_6 & 0 & 0 & 0 \\ 0 & 0 & 0 & 0 & 0 & 0 & I_1 & 0 & 0 \\ 0 & 0 & 0 & 0 & 0 & 0 & 0 & I_2 & 0 \\ 0 & 0 & 0 & 0 & 0 & 0 & 0 & 0 & I_3 \end{bmatrix} \bullet \begin{bmatrix} \ddot{x}_1 \\ \ddot{x}_2 \\ \ddot{x}_3 \\ \ddot{x}_4 \\ \ddot{x}_5 \\ \ddot{x}_6 \\ \ddot{\theta}_1 \\ \ddot{\theta}_2 \\ \ddot{\theta}_3 \end{bmatrix} +$$

$$\alpha \begin{bmatrix} (k_1+k_2) & -(k_1+k_2) & 0 & 0 & 0 & 0 & (k_1l_1-k_2l_2) & (k_2l_4-k_1l_3) & 0 \\ -(k_1+k_2) & \begin{pmatrix} k_1+k_2+k_3 \\ +k_4+k_7 \end{pmatrix} & -k_3 & -k_4 & -k_7 & 0 & (-k_1l_1+k_2l_2) & \begin{pmatrix} k_3l_5-k_4l_6+k_1l_3 \\ -k_2l_4-k_7l_7 \end{pmatrix} & -k_7l_8 \\ 0 & -k_3 & (k_5+k_3) & 0 & 0 & 0 & 0 & -k_3l_5 & 0 \\ 0 & -k_4 & 0 & (k_4+k_6) & 0 & 0 & 0 & k_4l_6 & 0 \\ 0 & -k_7 & 0 & 0 & (k_7+k_8) & -k_8 & 0 & k_7l_7 & (k_7l_8-k_8l_9) \\ 0 & 0 & 0 & 0 & -k_8 & (k_9+k_8) & 0 & 0 & k_8l_9 \\ (k_1l_1-k_2l_2) & (-k_1l_1+k_2l_2) & 0 & 0 & 0 & 0 & (k_1l_1^2+k_2l_2^2) & (-k_1l_1l_3-k_2l_2l_4) & 0 \\ (k_2l_4-k_1l_3) & \begin{pmatrix} k_3l_5-k_4l_6+k_1l_3 \\ -k_2l_4-k_7l_7 \end{pmatrix} & -k_3l_5 & k_4l_6 & k_7l_7 & 0 & (-k_1l_1l_3-k_2l_2l_4) & \begin{pmatrix} k_3l_5^2+k_2l_4^2+k_7l_7^2 \\ +k_4l_6^2+k_1l_3^2 \end{pmatrix} & k_7l_7l_8 \\ 0 & -k_7l_8 & 0 & 0 & (k_7l_8-k_8l_9) & k_8l_9 & 0 & k_7l_7l_8 & (k_7l_8^2+k_8l_9^2) \end{bmatrix} .. \begin{bmatrix} \dot{x}_1 \\ \dot{x}_2 \\ \dot{x}_3 \\ \dot{x}_4 \\ \dot{x}_5 \\ \dot{x}_6 \\ \dot{\theta}_1 \\ \dot{\theta}_2 \\ \dot{\theta}_3 \end{bmatrix}$$

$$+ \begin{bmatrix} (k_1+k_2) & -(k_1+k_2) & 0 & 0 & 0 & 0 & (k_1l_1-k_2l_2) & (k_2l_4-k_1l_3) & 0 \\ -(k_1+k_2) & \begin{pmatrix} k_1+k_2+k_3 \\ +k_4+k_7 \end{pmatrix} & -k_3 & -k_4 & -k_7 & 0 & (-k_1l_1+k_2l_2) & \begin{pmatrix} k_3l_5-k_4l_6+k_1l_3 \\ -k_2l_4-k_7l_7 \end{pmatrix} & -k_7l_8 \\ 0 & -k_3 & (k_5+k_3) & 0 & 0 & 0 & 0 & -k_3l_5 & 0 \\ 0 & -k_4 & 0 & (k_4+k_6) & 0 & 0 & 0 & k_4l_6 & 0 \\ 0 & -k_7 & 0 & 0 & (k_7+k_8) & -k_8 & 0 & k_7l_7 & (k_7l_8-k_8l_9) \\ 0 & 0 & 0 & 0 & -k_8 & (k_9+k_8) & 0 & 0 & k_8l_9 \\ (k_1l_1-k_2l_2) & (-k_1l_1+k_2l_2) & 0 & 0 & 0 & 0 & (k_1l_1^2+k_2l_2^2) & (-k_1l_1l_3-k_2l_2l_4) & 0 \\ (k_2l_4-k_1l_3) & \begin{pmatrix} k_3l_5-k_4l_6+k_1l_3 \\ -k_2l_4-k_7l_7 \end{pmatrix} & -k_3l_5 & k_4l_6 & k_7l_7 & 0 & (-k_1l_1l_3-k_2l_2l_4) & \begin{pmatrix} k_3l_5^2+k_2l_4^2+k_7l_7^2 \\ +k_4l_6^2+k_1l_3^2 \end{pmatrix} & k_7l_7l_8 \\ 0 & -k_7l_8 & 0 & 0 & (k_7l_8-k_8l_9) & k_8l_9 & 0 & k_7l_7l_8 & (k_7l_8^2+k_8l_9^2) \end{bmatrix} .. \begin{bmatrix} x_1 \\ x_2 \\ x_3 \\ x_4 \\ x_5 \\ x_6 \\ \theta_1 \\ \theta_2 \\ \theta_3 \end{bmatrix} = \begin{bmatrix} \mathbf{0} \\ \mathbf{0} \\ \boldsymbol{F_1} \\ \boldsymbol{F_2} \\ \mathbf{0} \\ \boldsymbol{F_3} \\ \mathbf{0} \\ \mathbf{0} \\ \mathbf{0} \end{bmatrix} \boldsymbol{e^{-jwt}} \qquad (17)$$

Table 1. Dimensions and stiffness data (Elmadany 1987).

	Driver cabin	Tractor (with engine)	Trailer	Un-sprung masses
Dimensions (m)	L_1=1.9 L_2=1.2	L_3=1.22 L_4=1.25 L_5=1.20 L_6=2.10 L_7=2.08	L_8=5.42 L_9=3.11	
Mass (kg)	M_1=1,932	M_2=4,508	M_4=3,660	M_3=360 M_5=1,450 M_6=1,450
Stiffness kN/m	K_1=150 K_2=150	K_3=357 K_4=630	K_7=6,000 K_8=630	K_5=1,560 K_6=5,250 K_9=5,250
Moments of inertia (kgm^2)		I_1=1017	I_2=2373	I_3=48,140
Damping *c* kNs/m *(Calculated with* 1/3,500 *factor)*		C_3=0.102 C_4=0.180	C_7=1.714 C_8=0.180	C_5=0.446 C_6=1.500 C_9=1.500

Results

The road excitation causes the vehicle to make linear deflections and angular tilting as shown in the following set of figures.

Modes of Vibration

There are 9 modes of vibration possible as shown in Fig. 3, the 7th, 8th, and 9th degrees of freedom are the angular tilts. The displacements were normalised with the maximum displacement.

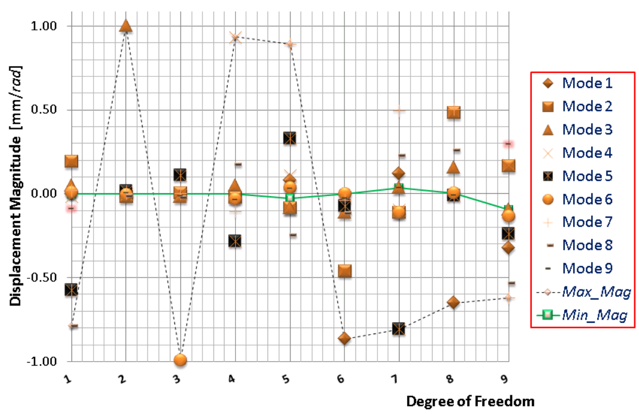

Fig. 3. Modes of vibration for vehicle.

The *Max_Mag* and *Min_Mag* in Fig. 3 represent the maximum and minimum magnitudes at the various modes of vibration. It also shows the phases of the degree of freedom in different modes relative to one another.

Dynamic Displacements

The vertical displacement of the vehicle is shown in Figs. 4 and 5.

Angular Tilt

The rotation or tilt of the compartments is shown in Fig. 6 and the driver cabin is shown in Fig. 7.

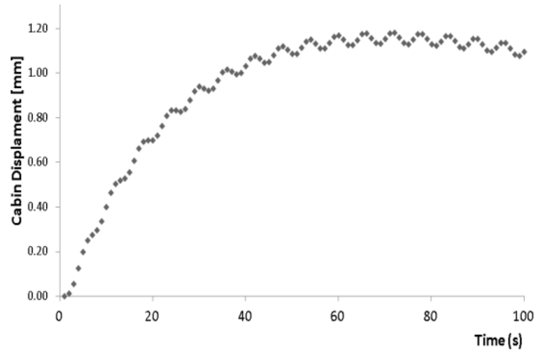

Fig. 4. Driver cabin dynamic displacement.

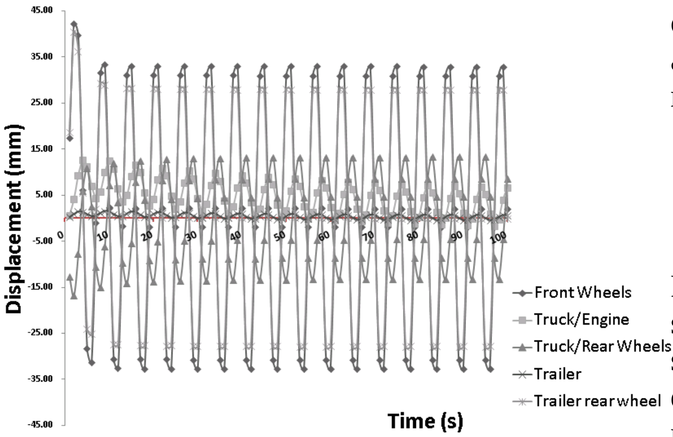

Fig. 5. Displacement with time of the vehicle parts.

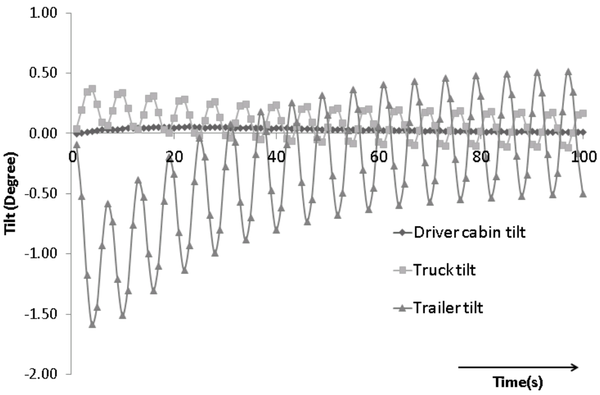

Fig. 6. Compartmental rotations.

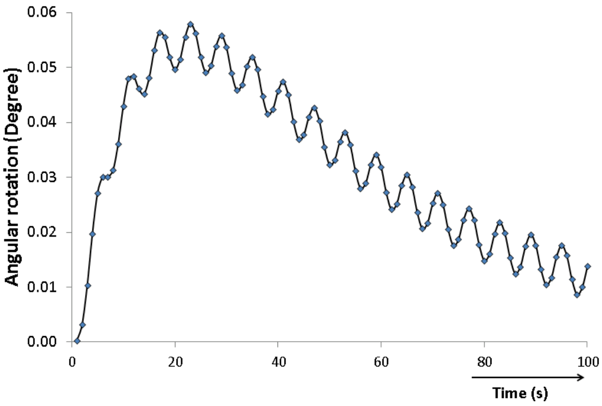

Fig. 7. Rotation of the driver cabin.

Driver Experience

The comfort of the driver can be measured as a function of force experienced as a result of the maximum impact. For a sinusoidal forcing function, the maximum is experienced at maximum acceleration given by:

$$a = \omega^2 A. \quad (18)$$

At the speed of 60 km/hr, the acceleration experienced is 1.32% *g*, where *g* = acceleration of gravity (9.80665 m/s^2); *a* = circular motion acceleration; and *A* is the amplitude of the motion.

Discussion

The maximum displacement, as shown in Fig. 5, is experienced by the front wheel and similarly by the trailer rear wheel in the first 5 seconds of impact on the rough road. The displacements do not go below 25 mm and not more than 35 mm over time.

The displacement of the cabin compartment, where the driver seat is located, grows from rest to only about 1 mm within the first 60 seconds and stays within this range over time. During the first 20 seconds, the maximum tilt experienced is only about 0.05^o and keeps oscillating at less than 0.02^o, while the trailer compartment oscillates to a maximum value of 1.5^o before reaching a stabilised oscillation of about 0.5^o after 60 seconds. The engine compartment experiences stability almost immediately at less than 0.5^o and maximum amplitude of 12 mm.

The driver experience is only 1.32% of *g* at the maximum, meaning that the driver experience as a result of driving the truck on the rough road is comfortable if measured as a result of impact and not the fatigue that can be experienced as a result of long time driving and low frequency vibrations.

In this simulation, the road is 0.1 m rough in crest and the whole system response is about 35 mm at the wheels and even less than 2 mm inside the compartments with less than 1.5^o, making it suitable for sensitive item transportation in a real case scenario.

Conclusion

The values of damping coefficients can be modelled as a function of the stiffness matrix to simplify the system of equations and to cater for the difficulty of measuring damping coefficients of a spring-mass system. Vehicle suspension designs (Fujishiro *et al*. 1987) may incorporate variable damping and this method can be used to approximate system response. A properly designed suspension system can absorb significant amount of shock to provide driving comfort. Selective choice of the suspension system can give selective comfort at different compartments in an articulated vehicle.

Acknowledgment

The authors would like to acknowledge the kind assistance of Dr. Paul Fromme, Department of Mechanical Engineering, Faculty of Engineering Science, University College London (UCL), London, England, UK, for the original base code which was modified to suit this analysis.

Nomenclature

Symbol	Use
j	Complex number
i	An integer index
I	Moment of Inertia (kg·m^2)
k	Stiffness (N/m)
l	Length (m)
g	Gravity (9.80665 m/s^2)
F	Force (N)
C	Coefficient of damping (N·s/m)

Greek symbols

Symbol	Meaning/Use
ω	Angular frequency (rad/s)
$\dot{\theta}_i$	Angular velocity (rad/s)
$\ddot{\theta}_i$	Angular acceleration (rad/s^2)

References

ElMadany, M.M. 1987. Nonlinear ride analysis of heavy trucks. Computers and Structures 25(1): 69-82.

Fan, Z.P.; Zeng, H.; Yang, J.W.; and Li, J. 2011. Study on decreasing vibration of high-speed train semi-active suspension system. Advanced Materials Research 230-232: 1,104-9.

Fujishiro, T.; Takahashi, S.; and Kaneko, T. 1987. Automotive suspension system with variable damping characteristics. United States Patent Office, US Patent 4,696,489, filed 13 January 1986, issued 29 September 1987.

Hać, A. 1985. Suspension optimization of a 2-DOF vehicle model using a stochastic optimal control technique. Journal of Sound and Vibration 100(3): 343-57.

Hedrick, J.K.; and Butsuen, T. 1990. Invariant properties of automotive suspensions. Proceedings of the Institution of Mechanical Engineers (IMechE), Part D: Journal of Automobile Engineering 204(1): 21-7.

Ikenaga, S.; Lewis, F.L.; Campos, J.; and Davis, L. 2000. Active suspension control of ground vehicle based on a full-vehicle model. Proceedings of the 2000 American Control Conference, 28-30 June 2000, Chicago, IL, USA. Vol. 6, pp. 4,019-24.

Jiang, Z.; Streit, D.A.; and El-Gindy, M. 2001. Heavy vehicle ride comfort: literature survey. International Journal of Heavy Vehicle Systems 8(3/4): 258-84.

Jie, H.; Yikai, C. Chihang, Z.; Zhiguo, Q.; and Xiuhuan, R. 2011. Heavy truck suspension optimisation based on modified skyhook damping control. International Journal of Heavy Vehicle Systems 18(2): 161-78.

M'Sirdi, N.K.; Rabhi, A.; Zbiri, N.; and Delanne, Y. 2005. Vehicle-road interaction modelling for estimation of contact forces. Vehicle System Dynamics 43(Supplement 1): 403-11.

Mabbot, N.; Foster, G.; and McPhee, B. 2001. Heavy Vehicle Seat Vibration and Driver Fatigue. Department of Transport and Regional Services, Australian Transport Safety Bureau, Canberra, Australia, Report No. CR 203.

Maeda, C.; Kawamura, A.; Shirakawa, T.; Nakatsuji, T.; and Kumada, K. 2005. Reproducibility of the vehicle vertical motion by KIT driving simulator using the actual measurement data. Journal of the Eastern Asia Society for Transportation Studies 6: 2,734-46.

Singiresu, S.R. 2004. Mechanical Vibrations. Pearson Education, Upper Saddle River, NJ, USA.